Clinical Cancer Research

Dual Inhibition of IGF-1R and ErbB3 Enhances the Activity of Gemcitabine and Nab-Paclitaxel in Preclinical Models of Pancreatic Cancer

Adam J. Camblin[1], Emily A. Pace[1], Sharlene Adams[1], Michael D. Curley[1], Victoria Rimkunas[1], Lin Nie[1], Gege Tan[1], Troy Bloom[1], Sergio Iadevaia[1], Jason Baum[1], Charlene Minx[2], Akos Czibere[1], Chrystal U. Louis[1], Daryl C. Drummond[1], Ulrik B. Nielsen[1], Birgit Schoeberl[1], J. Marc Pipas[1], Robert M. Straubinger[2,3], Vasileios Askoxylakis[1], and Alexey A. Lugovskoy[1]

Abstract

Purpose: Insulin-like growth factor receptor 1 (IGF-1R) is critically involved in pancreatic cancer pathophysiology, promoting cancer cell survival and therapeutic resistance. Assessment of IGF-1R inhibitors in combination with standard-of-care chemotherapy, however, failed to demonstrate significant clinical benefit. The aim of this work is to unravel mechanisms of resistance to IGF-1R inhibition in pancreatic cancer and develop novel strategies to improve the activity of standard-of-care therapies.

Experimental Design: Growth factor screening in pancreatic cancer cell lines was performed to identify activators of prosurvival PI3K/AKT signaling. The prevalence of activating growth factors and their receptors was assessed in pancreatic cancer patient samples. Effects of a bispecific IGF-1R and ErbB3 targeting antibody on receptor expression, signaling, cancer cell viability and apoptosis, spheroid growth, and *in vivo* chemotherapy activity in pancreatic cancer xenograft models were determined.

Results: Growth factor screening in pancreatic cancer cells revealed insulin-like growth factor 1 (IGF-1) and heregulin (HRG) as the most potent AKT activators. Both growth factors reduced pancreatic cancer cell sensitivity to gemcitabine or paclitaxel in spheroid growth assays. Istiratumab (MM-141), a novel bispecific antibody that blocks IGF-1R and ErbB3, restored the activity of paclitaxel and gemcitabine in the presence of IGF-1 and HRG *in vitro*. Dual IGF-1R/ErbB3 blocking enhanced chemosensitivity through inhibition of AKT phosphorylation and promotion of IGF-1R and ErbB3 degradation. Addition of istiratumab to gemcitabine and nab-paclitaxel improved chemotherapy activity *in vivo*.

Conclusions: Our findings suggest a critical role for the HRG/ErbB3 axis and support the clinical exploration of dual IGF-1R/ErbB3 blocking in pancreatic cancer. *Clin Cancer Res; 24(12); 2873–85. ©2018 AACR.*

Introduction

Pancreatic cancer remains a leading cause of cancer mortality (1). The 5-year overall survival (OS) rate for pancreatic ductal adenocarcinoma (PDAC) is only 5% to 10% (2). The most effective first-line treatments for patients with metastatic disease include a combination of gemcitabine with nab-paclitaxel (3), and a four-drug combination, consisting of leucovorin, fluorouracil, irinotecan, and oxaliplatin (FOLFIRINOX; ref. 4). Median overall survival (mOS) with these regimens is 8.5 and 11.1 months, respectively (3, 4). Despite the largest increase in survival for FOLFIRINOX, this regimen is characterized by substantial toxicity and is usually restricted to patients with good performance status. Recently, nanoliposomal irinotecan (Onivyde), in combination with fluorouracil and leucovorin, was approved by the US Food and Drug Administration for the treatment of patients with metastatic disease who previously received gemcitabine-based therapy (5, 6). Although this combination extends survival and has a manageable safety profile, mOS is 6.1 months (6). Therefore, there remains an urgent need for novel therapies with better efficacy to further improve patient outcomes in this deadly neoplasm.

Insulin-like growth factor receptor 1 (IGF-1R) is a receptor tyrosine kinase (RTK) that has a key role in cancer pathophysiology, promoting cancer cell survival and proliferation, tumor growth, and therapeutic resistance (7, 8). Ligands of IGF-1R may be delivered through endocrine or autocrine/paracrine signaling in aggressive cancers (9). Increased levels of insulin-like growth factor-1 (IGF-1) are associated with enhanced cancer risk and resistance to chemotherapies across multiple cancer indications; including esophageal, colon, breast, prostate, and lung cancers (10–15). High levels of IGF-1 and IGF binding proteins have been detected in the blood of patients with pancreatic cancer,

[1]Merrimack Pharmaceuticals, Inc., Cambridge, Massachusetts. [2]Department of Pharmaceutical Sciences, State University of New York at Buffalo, Buffalo, New York. [3]Department of Pharmacology and Therapeutics, Roswell Park Comprehensive Cancer Center, Buffalo, New York.

Note: Supplementary data for this article are available at Clinical Cancer Research Online (http://clincancerres.aacrjournals.org/).

A.J. Camblin, E.A. Pace, and S. Adams are equally contributing first authors.

V. Askoxylakis and A.A. Lugovskoy are equally contributing senior authors.

Corresponding Author: Adam J. Camblin, Merrimack Pharmaceuticals (United States), One Kendall Square, Building 700 Fl 2, Cambridge, MA 02139. Phone: 617-441-1000; Fax: 617-491-1386; E-mail: acamblin@merrimack.com; and Vasileios Askoxylakis, VAskoxylakis@merrimack.com

doi: 10.1158/1078-0432.CCR-17-2262

Translational Relevance

Metastatic pancreatic cancer remains a leading cause of cancer mortality. High levels of IGF-1R in pancreatic cancer are associated with higher tumor grade and decreased survival. However, IGF-1R inhibitors have failed to show significant clinical benefit. Our studies show that the HRG/ErbB3 axis is critical to pancreatic cancer progression and therapeutic resistance to IGF-1R inhibition. Both IGF-1R and ErbB3 can serve as drivers of tumor growth and resistance/tolerance to standard-of-care chemotherapy. Dual targeting of the IGF-1R and ErbB3 pathways with the novel bispecific antibody istiratumab increases the activity of standard-of-care chemotherapies. These data provide mechanistic insight into pancreatic cancer resistance to IGF-1R inhibitors and identify novel translatable treatment strategies for the disease.

correlating with enhanced IGF-1R phosphorylation in tumor tissue (16). High expression of IGF-1R in pancreatic cancer is associated with higher tumor grade and decreased survival (17). This provided the rationale for the development and clinical testing of IGF-1R inhibitors in pancreatic cancer. However, despite evidence that IGF-1R pathway signaling is implicated in tumor progression, as well as promising early-phase clinical data with IGF-1R targeting antibodies (18, 19), larger phase III clinical trials failed to show an advantage of targeting IGF-1R in pancreatic cancer (20).

Resistance to IGF-1R targeted therapies remains a major challenge. Mechanisms of resistance include a compensatory re-activation of downstream PI3K/AKT/mTOR signaling (21). This hypothesis is supported by findings in various cancer types, which reveal an interplay between IGF-1R and other RTKs (22–25). Preclinical studies have shown that IGF-1R inhibition upregulates insulin receptor signaling in malignancies (19, 21, 26), whereas further studies suggest that ErbB receptor signaling confers resistance to IGF-1R inhibition (21, 23).

Despite the well-characterized implications of IGF-1R signaling in pancreatic cancer, knowledge and understanding of resistance to IGF-1R inhibitors in pancreatic tumors are limited. This study sought to identify potent activators of pancreatic cancer cell survival and growth, determine pathways that promote desensitization to gemcitabine and paclitaxel, and reveal strategies to re-sensitize pancreatic cancer cells to standard of care treatment. Our data highlight the role of the HRG/ErbB3 axis in pancreatic cancer and the therapeutic potential of dual IGF-1R/ErbB3 inhibition in this setting, supporting the clinical exploration of a novel bispecific IGF-1R/ErbB3 inhibitor as a therapeutic for the treatment of pancreatic cancer.

Materials and Methods

Cell lines and reagents

All cell lines in this study were obtained from the ATCC, except KP-4 (RIKEN Bioresources Cell Bank). Cell lines were confirmed negative for mycoplasma prior to use, maintained according to manufacturer recommendations (Supplementary Table S1) and propagated for less than 8 weeks after initial plating. All recombinant human growth factors were obtained from PeproTech, except IGF-1 (R&D Systems), HRG (R&D Systems), and insulin (Sigma) as described in Supplementary Table S2.

In vitro signaling experiments

Unless otherwise mentioned, cells were seeded into 96-well tissue culture plates (Costar) at 20,000 cells/well in complete media supplemented with 10% FBS. The following day, cells were synchronized by 24-hour serum starvation in media with 2% FBS. Signaling experiments were stopped with a cold PBS wash, and cell lysates were generated with Mammalian Protein Extraction Reagent (Thermo Scientific) supplemented with phosphatase and protease inhibitor pellets (Roche) and 150 mmol/L sodium chloride (Sigma). For receptor ubiquitination experiments, cells were seeded into 15 cm dishes, pretreated with the proteasome inhibitor epoxomicin (Sigma) for 2 hours, and treated as indicated. Cells were harvested and cell lysates clarified by centrifugation at 13,000 rpm at 4°C. Receptors were immediately immunoprecipitated using Dynabeads (Life Technologies) with IGF-1R (Cell Signaling Technology) or ErbB3 (R&D Systems) antibodies. For gemcitabine- and paclitaxel-induced upregulation of IGF-1R and ErbB3 receptors, cells were seeded into 10-cm dishes and lysates were clarified by centrifugation at 13,000 rpm for 10 minutes at 4°C.

Caspase-3/7 cleavage activity experiments

Cells were seeded into 96-well tissue culture plates at 5,000 cells per well in media containing 2% FBS. The following day, media was replaced with media containing 2% FBS and the Essen BioSciences IncuCyte Caspase-3/7 Green Apoptosis Assay Reagent (catalog no. 4440), then immediately treated in octuplicate as indicated. Caspase-3/7 activity was measured 16 hours following start of treatment in the IncuCyte imager, and then normalized to cell density within each well.

ELISA

ELISAs were performed as described previously (17). Briefly, high-binding assay plates (Corning) were coated with capture antibodies and incubated overnight followed by blocking with 2% BSA (Sigma) in PBS for 1 hour. Plates were incubated with lysate diluted 2-fold in 2% BSA, 0.1% Tween-20 PBS for 2 hours, then with primary detection antibodies for 2 hours, followed by secondary detection antibodies for 30 minutes. Chemiluminescent substrate (Pierce) was added to each plate for 20 minutes and luminescence measured using a Synergy H1 plate reader. Plates were washed four times with a PBS solution containing 0.05% Tween-20 between each incubation, and all incubations were done at room temperature. See Supplementary Table S3 for antibody information.

Western blot analysis

Samples were analyzed by Western blotting as described previously (13). Briefly, clarified cell lysates were boiled in LDS sample buffer (Life Technologies) at 95°C for 5 minutes, and resolved by electrophoresis on 4%–12% gels (Bio-Rad) using MES running buffer (Bio-Rad). Proteins were transferred to nitrocellulose membranes (Life Technologies) using an iBlot device (Life Technologies) and membranes were blocked in blocking buffer (LI-COR Biosciences) for 1 hour at room temperature. Membranes were probed with primary antibodies in 5% BSA (Sigma), 0.1% Tween-20 Tris-buffered saline solution (TBS-T) overnight at 4–8°C, washed three times for 10 minutes in TBS-T,

followed by incubation with an anti-rabbit secondary antibody (Licor) in 5% milk (Cell Signaling Technology) TBS-T for 45 minutes. After three additional 5-minute washes in TBS-T, bands were visualized on a LI-COR ODYSSEY CLx imager. Protein bands were quantified using Image Studio (version 3.1.4) software.

Tumor spheroid growth assay

Cells were seeded into 96-well nano-culture plates (SCIVAX) at 5,000 cells/well and treated following 24-hour growth in media containing 2% FBS. Cell proliferation was measured using Cell Titer-Glo Luminescent Cell Viability Assay Kit (Promega) according to the manufacturer's instructions. Luminescence was measured using a Synergy H1 plate reader.

Cell line–derived xenograft studies

All animal studies were performed according to the guidelines and approval of the Institutional Animal Care and Use Committee. Female Fox Chase SCID Beige mice were obtained from Charles River Laboratories and were housed in a pathogen-free environment under controlled conditions and received food and water ad libitum. Tumors were established by subcutaneous injection of 5×10^6 cells, suspended in 200 μL of 1:1 Matrigel (Corning): unsupplemented culture media, into one shaven flank of recipient mice. Once the average measured tumor volume [calculated according to the formula: $\pi/6 \times (\text{length} \times \text{width} \times \text{width})$] had reached approximately 400 mm^3, mice were randomized into groups and treatment was administered as outlined in figure legends. The average starting tumor volume per group was equivalent across all groups. Tumor volumes were measured twice weekly and statistical significance of mean tumor volume comparisons are represented as *P* values calculated using two-sided, two-sample equal variance *t* tests. For pharmacodynamic analyses, tumors were snap-frozen in liquid nitrogen immediately upon extraction, pulverized in a CryoPrep pulverizer (Covaris), and resuspended in Tissue Protein Extraction Reagent (Life Technologies) supplemented with phosphatase and protease inhibitor pellets (Roche). Following 30-minute incubation on ice, crude tumor lysates were transferred to Qiashredder tubes (Qiagen) and clarified by centrifugation (13,000 rpm, 4°C) for 10 minutes.

Patient-derived xenograft studies

All animal studies were performed according to the guidelines and approval of the Institutional Animal Care and Use Committee. C.B-Igh-1b/lcrTac-Prkdcscid mice were obtained from the Roswell Park Comprehensive Cancer Center, Department of Laboratory Animals Colony, and were housed in a pathogen-free environment under controlled conditions and received food and water ad libitum. Tumors used for the study were grown in a donor mouse to a volume of approximately 1,500 mm^3. Once the tumor reached that volume, the tumor was harvested, cut into 2 mm^3 pieces, inserted subcutaneously into the right flank of each mouse, and the skin was closed with a wound clip. Wound clips were removed 10–14 days postimplantation and tumors were measured 1–2 times per week. Once the average measured tumor volume (calculated according to the formula: $(\text{length} \times \text{width} \times \text{height})/2$) had reached approximately 400 mm^3, mice were randomized into groups and treatment was administered as outlined in the figure legends. The average starting tumor volume per group was equivalent across all groups. Tumor volumes were measured twice weekly and statistical significance of differences in mean tumor volumes are represented as *P* values calculated using two-sided *t* tests.

Histology of tumor tissue

Metastatic PDAC tumor biopsies were commercially sourced from Avaden Biosciences. All tumor tissue samples were formalin fixed, paraffin-embedded, sectioned to 4- to 5-μm thickness, and analyzed using the Leica Bond Rx or Ventana Benchmark Discovery Platforms. Antibodies used for IHC were as follows: anti-IGF-1R (Ventana, G11), anti-ErbB3 (Cell Signaling Technology, D22C5). All IHC-stained specimens were scored by a board-certified clinical pathologist utilizing the clinical HER2 scoring system. Detection of IGF-1 (#313037), IGF-2 (#594367), and HRG (#311187) transcripts was performed using the *in situ* hybridization RNAscope automated assay for the Leica Bond Rx (#321100) in accordance with protocols provided by Advanced Cell Diagnostics. For each tissue specimen, positive (PPIB, #313907) and negative (DapB, #312037) control RNA probes were evaluated to assess tissue quality and assay performance alongside scoring of each individual target probe, and scoring was based on counting dots per cell.

Statistical analysis

Statistical significance for *in vitro* results was determined by two-way ANOVA/Tukey multiple comparison test using GraphPad Prism software, and statistical significance between mean xenograft tumor volumes are represented as *P* values calculated using two-sided, two-sample equal variance *t* tests using Microsoft Excel software.

Results

IGF1 and HRG potently activate prosurvival signaling in pancreatic cancer

To investigate the relative importance of various potential activators of PI3K/AKT/mTOR signaling in pancreatic cancer, we determined AKT phosphorylation in response to a diverse panel of growth factors in nine PDAC cancer cell lines (Supplementary Tables S1 and S2). AKT phosphorylation was determined by Western blot analysis (Fig. 1A) and ELISA (Fig. 1B). Both analyses showed that IGF-1 and/or HRG induced the highest AKT phosphorylation in all cell lines (Fig. 1; Supplementary Fig. S1). HRG was found to cause the strongest AKT activation in all but two of the pancreatic cancer cell lines (PANC-1 and KP-4). Both PANC-1 and KP-4 cells were most responsive to IGF-1. Investigation of cell surface IGF-1R and ErbB3 receptor expression as measured by quantitative flow cytometry revealed a variable expression of IGF-1R and ErbB3 throughout the PDAC cell line panel (Fig. 1C).

The prevalence of IGF-1R, ErbB3, and their respective ligands (IGF-1, IGF-2, and HRG) was investigated in biopsies or surgical resections from pancreatic cancer patients with stage IV metastatic disease (Fig. 2A–O). Expression of IGF-1R and ErbB3 in the human samples was investigated by IHC, whereas expression of IGF-1, IGF-2, and HRG was investigated by RNA *in situ* hybridization (RNA-ISH). IGF-1R was detectable in 56% of PDAC human tumors, whereas ErbB3 was detectable in 61% of the tumors (Fig. 2P). Detectable levels of either IGF-1R or ErbB3 were measured in 83% of the analyzed samples. IGF-1, IGF-2, and HRG

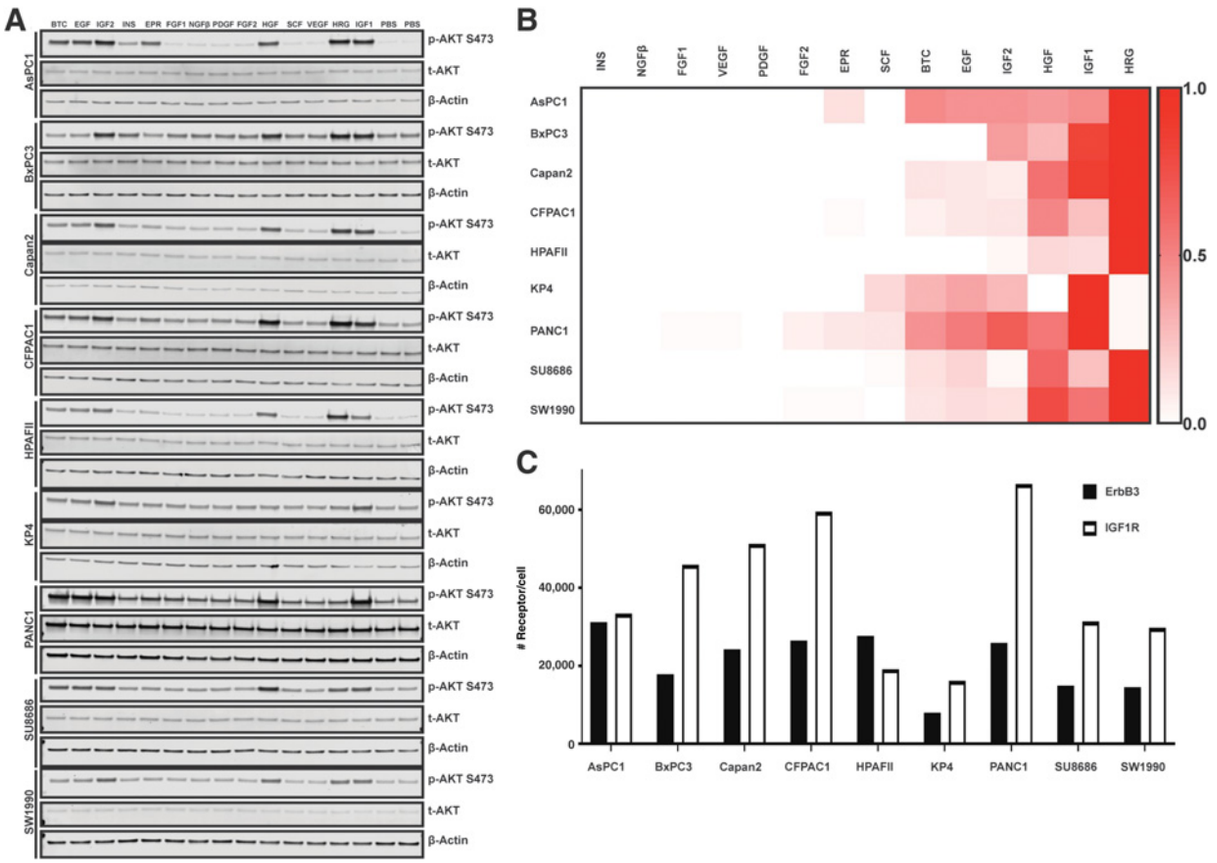

Figure 1.

IGF-1 and HRG induce AKT phosphorylation in pancreatic cancer cells. **A,** Nine pancreatic cancer cell lines were serum-starved for 24 hours and then treated for 15 minutes with 100 ng/mL of each growth factor. Cell lysates were collected, and pAKT S473 was determined by Western blot analysis (**A**) or ELISA (**B**). For ELISA, ng/mL pAKT was control-subtracted and maximum-normalized within each cell line. Heatmap data represent mean normalized values of duplicates from two separate experiments. **C,** Surface IGF-1R and ErbB3 receptor levels were quantified in nine human pancreatic cell lines using quantitative flow cytometry. Data represent number of receptors/cell from two separate experiments.

mRNA was detected by RNA *in situ* hybridization in 33%, 69%, and 43% of PDAC tumors, respectively (Fig. 2P). Fifty-six percent of samples were found to express IGF-1 or HRG. Coprevalence of IGF-1R and ErbB3 was found in 39% of samples. Coprevalence of IGF-1 and HRG was found in 26% of samples, whereas 40% of samples showed a coprevalence of IGF-2 and HRG. All three ligands (IGF-1, IGF-2, and HRG) were detected in 23% of the tested samples. Together, these data suggest that IGF-1R and/or ErbB3 signaling pathways may be active in many patients with pancreatic cancer.

Dual IGF-1R/ErbB3 blockade inhibits growth factor–induced prosurvival signaling in pancreatic cancer

On the basis of the finding that HRG and IGF-1 are strong activators of AKT in pancreatic cancer cells, we hypothesized that dual blocking of IGF-1R and ErbB3 can effectively inhibit growth factor–mediated prosurvival signaling. We tested the ability of the tetravalent bispecific antibody istiratumab to inhibit AKT activation in nine pancreatic cancer cell lines in response to stimulation with IGF-1, HRG, or costimulation with both IGF-1 and HRG. Istiratumab significantly inhibited AKT activation in response to IGF-1 and HRG costimulation in all cell lines (Fig. 3A; Supplementary Fig. S2). This was the case both when cells were exposed to istiratumab prior to ligand (Fig. 3A) and when cells were exposed to ligand prior to the antibody (Supplementary Fig. S2). Of note, istiratumab also inhibited IGF-1- and HRG-induced AKT phosphorylation in pancreatic cancer cells that harbor activating *KRAS* mutations, such as HPAF-II (KRAS G12V) and CFPAC-1 (KRAS G12D).

To determine the impact of the bispecific antibody format, we compared AKT phosphorylation in HPAF-II and CFPAC-1 cells in the presence of istiratumab or a mixture of IGF-1R- and ErbB3-targeting monospecific antibodies. Our studies showed that 500 nmol/L istiratumab was superior in inhibiting *in vitro* AKT phosphorylation, compared with the mixture of 500 nmol/L IGF-1R- and 500 nmol/L ErbB3-targeting mAbs (Fig. 3B). Mechanistic analyses revealed that istiratumab decreased IGF-1R and/or ErbB3 protein levels in nearly all nine pancreatic cancer cell lines tested (Fig. 4A). Moreover, istiratumab decreased IGF-1R and ErbB3 to a greater extent than either IGF-1R- or ErbB3-targeting monospecific

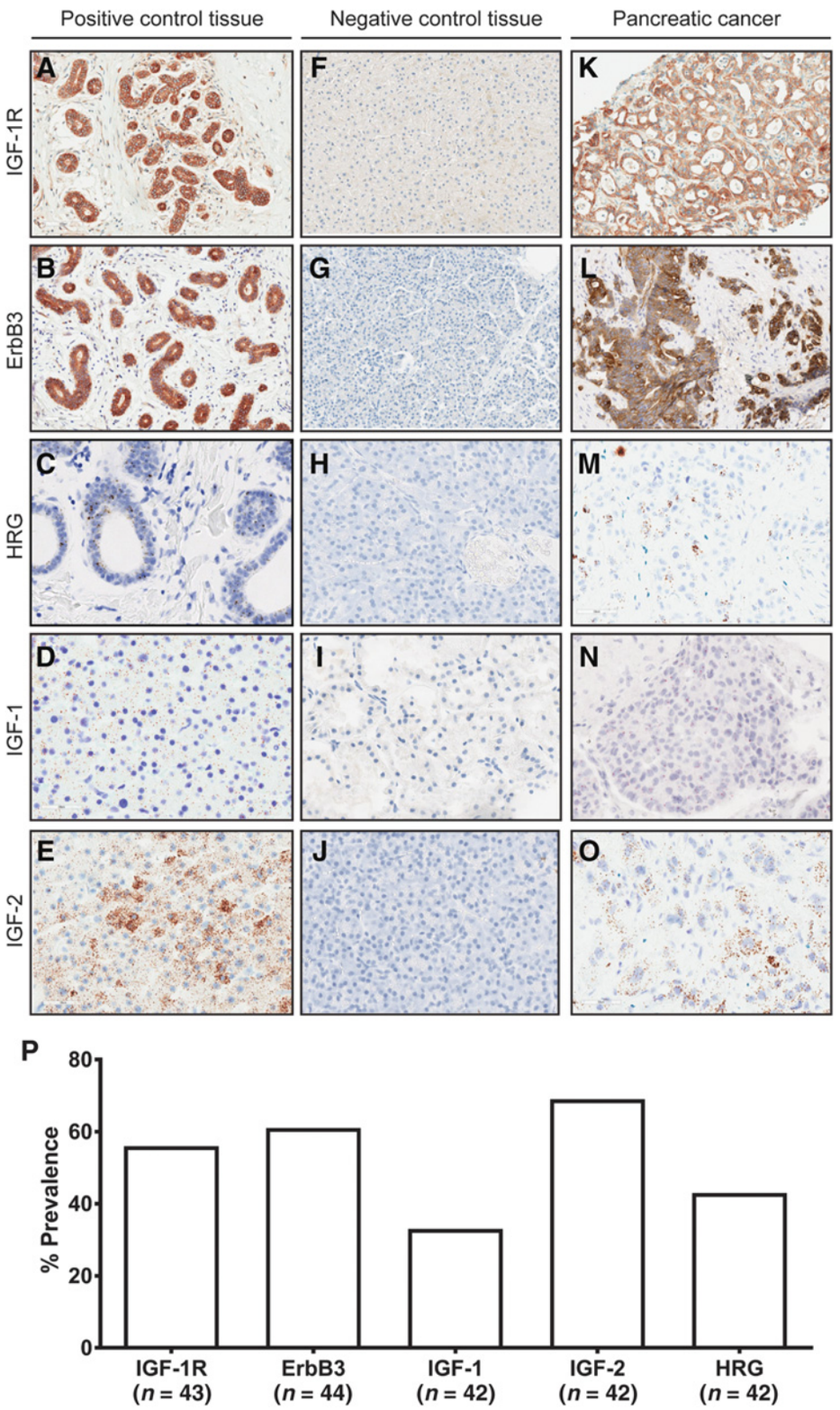

Figure 2.
Expression of IGF-1R, ErbB3, and their ligands (IGF-1, IGF-2, and HRG) in human metastatic pancreatic cancer tissue. **A–O,** Representative images of IGF-1R and ErbB3 IHC (diffuse brown staining) and representative images of IGF-1, IGF-2, and HRG RNA *in situ* hybridization (RNA-ISH, punctate dots in cells) from pancreatic cancer tissues are shown next to normal control tissues. Positive and negative controls include normal breast tissue (**A–C**), normal liver tissue (**D–F**), normal pancreas tissue (**G–H, J**), and normal kidney tissue (**I**). **P,** A panel of metastatic pancreatic tumors was profiled for expression of IGF-1R, ErbB3, and their respective ligands. IHC specimens were scored by a pathologist using the clinical HER2 scoring system criteria (IHC positivity is considered $\geq$1+ in 10% of tumor cells), and ISH specimens were scored by quantifying dots/cell (ISH positivity is considered $\geq$1 dot/cell in at least 10% of tumor or stromal cells).

antibodies or their mixture in multiple cell lines (Fig. 4B and C). Monospecific anti-IGF-1R antibodies caused a compensatory increase in ErbB3 protein expression in Capan-2 cells (Fig. 4C), whereas anti-ErbB3 antibodies caused a compensatory increase in IGF-1R protein levels in Capan-2, CFPAC-1, and PANC-1 cells (Fig. 4B). Immunoprecipitation analysis of

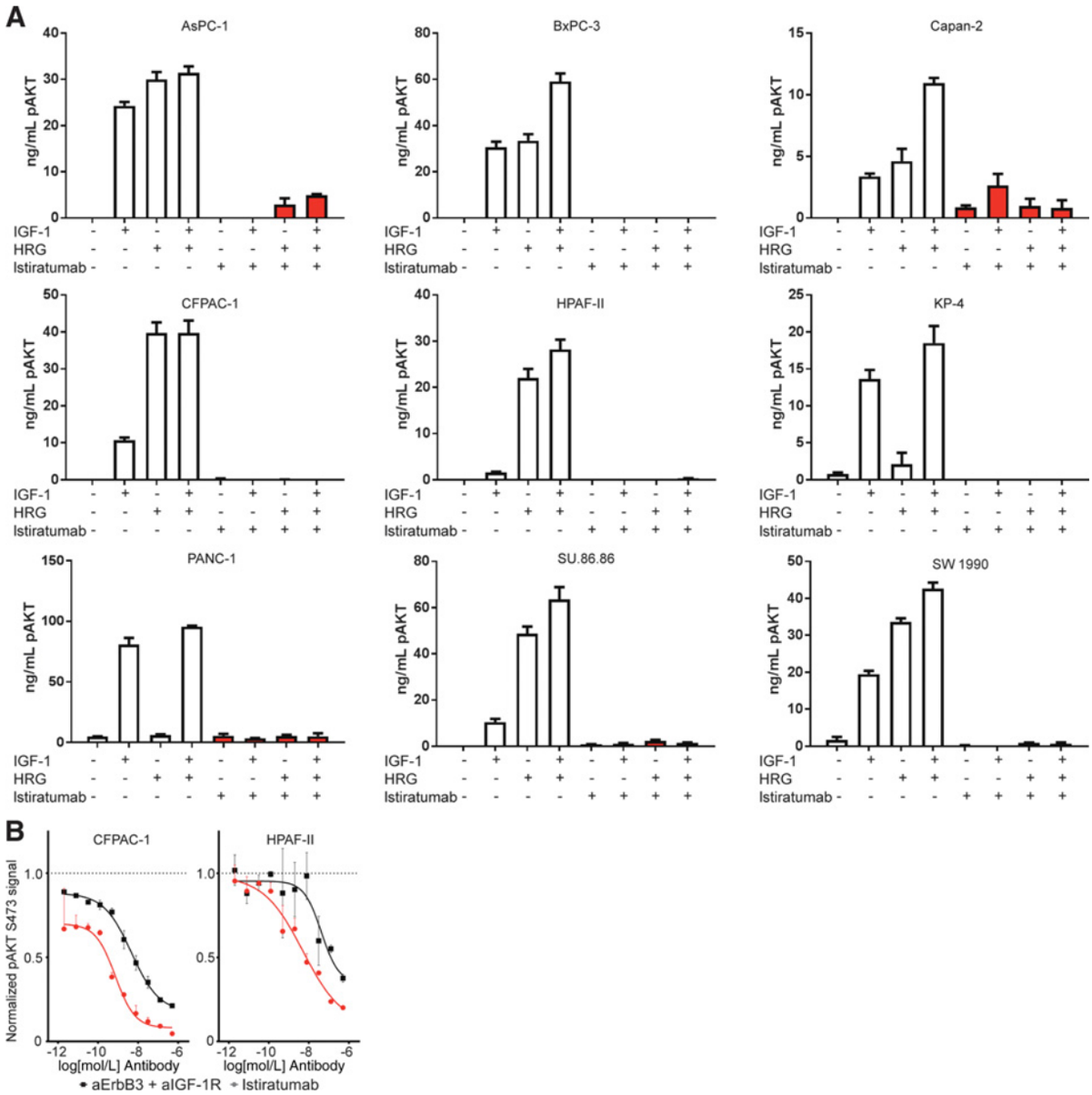

Figure 3.

Dual IGF-1R/ErbB3 blockade inhibits IGF-1– and HRG-induced AKT phosphorylation in human pancreatic cancer cell lines *in vitro*. **A,** Istiratumab inhibits dual growth factor–induced pAKT across the entire pancreatic cancer panel. Nine human pancreatic cancer cell lines were pretreated for 24 hours with vehicle or 500 nmol/L istiratumab, then stimulated for 15 minutes with a mixture of 50 nmol/L IGF-1 and 5 nmol/L HRG. Following treatment, cell lysates were collected and pAKT was measured by ELISA. Bars represent mean + SD of duplicates and are representative of a minimum of two separate experiments. **B,** Istiratumab inhibits dual growth factor–induced AKT phosphorylation stronger than a mixture of anti-IGF-1R and anti-ErbB3 monospecific antibodies. CFPAC-1 and HPAF-II cells were pretreated for 24 hours with a dilution series starting at 500 nmol/L of either istiratumab (red) or a mixture of anti-IGF-1R and anti-ErbB3 antibodies (black), then stimulated for 15 minutes with a mixture of 50 nmol/L IGF-1 and 5 nmol/L HRG. Following treatment, cell lysates were collected and pAKT was measured by ELISA. pAKT signal is control-subtracted and normalized to the IGF-1 + HRG control for each cell line. Line graphs are representative of the mean of two separate experiments, and are plotted as mean + SD of ELISA duplicates.

CFPAC-1 cell lysates revealed that treatment with istiratumab induced IGF-1R and ErbB3 receptor ubiquitination within 20 minutes, suggesting that istiratumab rapidly induces IGF-1R and ErbB3 receptor degradation through the proteasome pathway (Supplementary Fig. S3).

Dual IGF-1R/ErbB3 blockade prevents IGF-1 and HRG from desensitizing pancreatic cancer cells to gemcitabine or paclitaxel

The effects of IGF-1R/ErbB3 signaling on the activity of clinically relevant chemotherapies in pancreatic cancer were tested

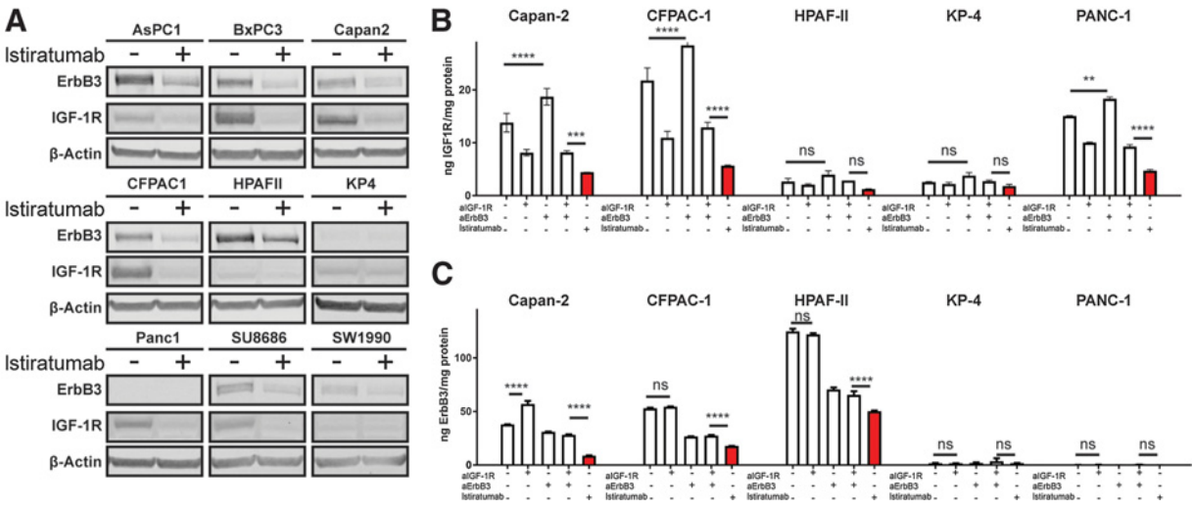

Figure 4.

Istiratumab induces receptor degradation stronger than anti-IGF-1R and anti-ErbB3 monospecific antibodies. **A,** Western blot analysis of ErbB3 and IGF-1R from cell lysates of nine pancreatic cancer cell lines after treatment in the absence or presence of istiratumab. **B** and **C,** Serum-starved pancreatic cancer cells were treated for 24 hours with vehicle, 500 nmol/L istiratumab, 500 nmol/L anti-IGF-1R antibody, or 500 nmol/L anti-ErbB3 antibody. Following treatment, cell lysates were harvested and total IGF-1R and ErbB3 levels were measured by ELISA. Bar graphs represent the mean + SD of ELISA duplicates and are representative of a minimum of two separate experiments. ns, not significant; **, $P < 0.005$; ***, $P < 0.001$; ****, $P < 0.0001$.

in vitro. Adding the growth factors IGF-1 and HRG reduced tumor cell sensitivity to paclitaxel or gemcitabine in spheroid growth assays (Fig. 5A and B; Supplementary Fig. S4). On the basis of our results showing that dual IGF-1R/ErbB3 blockade with istiratumab inhibits growth factor–induced activation of prosurvival signaling, we investigated whether istiratumab could resensitize pancreatic cancer cells to chemotherapy in the presence of IGF-1 and HRG. Our studies showed that the addition of istiratumab resensitized pancreatic cancer cells to paclitaxel or gemcitabine (Fig. 5A and B; Supplementary Fig. S4). Together, these data suggest that the IGF-1R and ErbB3 pathways are potential routes for escape of pancreatic cancer cells from gemcitabine and paclitaxel activity and that addition of istiratumab may restore sensitivity to these chemotherapy agents.

To determine potential interactions between chemotherapy and IGF-1R/ErbB3 pathways, we investigated the effects of gemcitabine and paclitaxel on IGF-1R and ErbB3 expression, as well as AKT phosphorylation. Both gemcitabine and paclitaxel promoted early (at 1-hour posttreatment) upregulation of IGF-1R and ErbB3 in CFPAC-1 cells (Fig. 5C and D). Paclitaxel induced an increase of AKT phosphorylation in the presence of IGF-1 or HRG (Fig. 5E and F). Gemcitabine also promoted a significant enhancement of AKT phosphorylation in the presence of HRG (Fig. 5F). Addition of istiratumab to either gemcitabine or paclitaxel in the presence of IGF-1 or HRG led to a striking decrease of pAKT (Fig. 5E and F). The changes in AKT phosphorylation correlated with changes in caspase-3/7 activity. IGF-1 and HRG led to a significant decrease of caspase-3/7 activity when added to paclitaxel chemotherapy *in vitro* (Fig. 5G and H). In the presence of IGF-1 and HRG, addition of istiratumab to gemcitabine or paclitaxel resulted in a significant increase of caspase activity (Fig. 5G and H) as compared with chemotherapy. Similar to observations with CFPAC-1, a chemotherapy-mediated increase in expression of IGF-1R and/or ErbB3 was measured in other pancreatic cancer cell lines (Supplementary Fig. S5).

These data demonstrate that treatment with gemcitabine and paclitaxel may alter the signaling network of pancreatic cancer cells in a manner that enhances IGF-1R and ErbB3 expression and subsequent AKT activation in response to IGF-1 and HRG. The data also suggest that istiratumab may potently inhibit AKT activation, resensitizing pancreatic cancer cells to chemotherapy and promoting apoptosis.

Dual IGF-1R/ErbB3 blockade potentiates the antitumor activity of chemotherapy *in vivo*

We tested whether adding istiratumab to gemcitabine and nab-paclitaxel increases the antitumor activity of chemotherapy in KRAS-mutant HPAF-II and CFPAC-1 cell line–derived xenograft models *in vivo*. Istiratumab monotherapy resulted in only a slight delay in tumor growth, whereas treatment with gemcitabine and nab-paclitaxel resulted in regression of CFPAF-I and strong growth delay of HPAF-II tumors (Fig. 6A and B). Addition of istiratumab to chemotherapy resulted in striking tumor regression in both models (Fig. 6A and B). Complete tumor eradication was detected in 40% and 20% of mice with HPAF-II and CFPAC-1 tumors, respectively, when istiratumab was added to chemotherapy. Pharmacodynamic analyses of CFPAC-1 and HPAF-II tumors showed that addition of istiratumab to gemcitabine and nab-paclitaxel decreased levels of IGF-1R and ErbB3 (Fig. 6C and D). Moreover, the triple combination decreased phosphorylation of ribosomal protein S6 and eukaryotic translation initiation factor 4E-binding protein 1 (4E-BP1), both downstream signaling of AKT, compared to the gemcitabine/nab-paclitaxel treatment (Figs. 6E–F). *In vivo* istiratumab-induced receptor downregulation was confirmed by IHC in both models (Fig. 6G). The *in vivo* pharmacodynamic effects of istiratumab over time were further investigated in HPAF-II xenograft tumor models. Here, tumors were harvested 16, 48, and 72 hours after a single treatment with istiratumab in combination with gemcitabine/nab-paclitaxel, and compared to tumors treated with gemcitabine/nab-paclitaxel alone. Western blot analysis

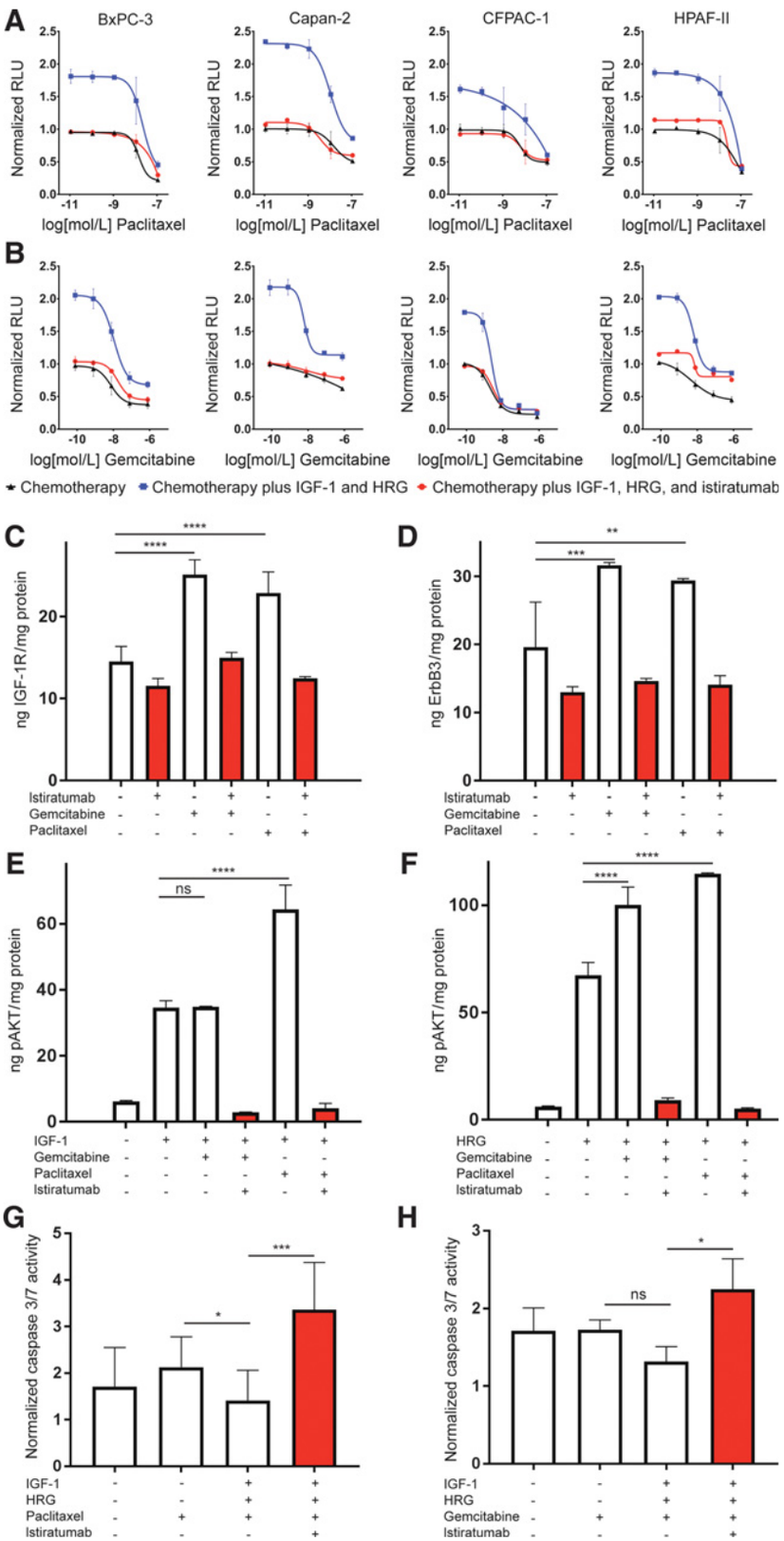

Figure 5.

Istiratumab restores activity of chemotherapy in the presence of IGF-1 and HRG. **A** and **B,** Serum-starved BxPC-3, Capan-2, CFPAC-1, and HPAF-II cell spheroids propagated in nanoculture plates were treated for 4 days with either paclitaxel (**A**) or gemcitabine (**B**) over a dilution series, in the presence of vehicle (blue), a mixture of 50 nmol/L IGF-1 and 10 nmol/L HRG (black), or a mixture of 50 nmol/L IGF-1, 10 nmol/L HRG, and 1 μmol/L istiratumab (red). Relative cell proliferation was assessed by CellTiter-Glo assay. Line graph data are expressed in relative light units (RLU) and are normalized to untreated vehicle (mean + SEM). **C** and **D,** Treatment with gemcitabine or paclitaxel upregulates IGF-1R and ErbB3 expression in CFPAC-1 pancreatic cancer cells. CFPAC-1 cells were treated for 1 hour with 1 μmol/L gemcitabine or 100 nmol/L paclitaxel. Cell lysates were collected, and IGF-1R and ErbB3 were quantified by ELISA. Bar graphs represent the mean + SD of duplicates and are representative of a minimum of two separate experiments. **E** and **F,** Istiratumab inhibits chemotherapy-enhanced, growth factor–induced AKT phosphorylation. CFPAC-1 cells were pretreated for 24 hours with either vehicle, 100 nmol/L paclitaxel (Pac), 1 μmol/L gemcitabine (Gem), 500 nmol/L istiratumab, alone or in combination as indicated, and then stimulated for 15 minutes with 50 nmol/L IGF-1 or 5 nmol/L HRG. Cell lysates were collected, and changes in pAKT were measured by ELISA. Bar graphs are plotted as the mean + SD of duplicates and are representative of a minimum of two separate experiments. **G** and **H,** Isitratumab potentiates chemotherapy-induced caspase-3/7 activity in the presence of IGF-1 and HRG. Serum-starved CFPAC-1 cells grown with the IncuCyte Caspase-3/7 Green Apoptosis Assay Reagent in 96-well plates were treated in octuplicate for 16 hours with 100 nmol/L paclitaxel (Pac), 1 μmol/L gemcitabine, 500 nmol/L istiratumab, 50 nmol/L IGF-1, or 5 nmol/L HRG as indicated, then caspase 3/7 activity was assessed in the IncuCyte live cell imager. ns, not significant; *, $P < 0.05$; **, $P < 0.005$; ***, $P < 0.001$; ****, $P < 0.0001$.

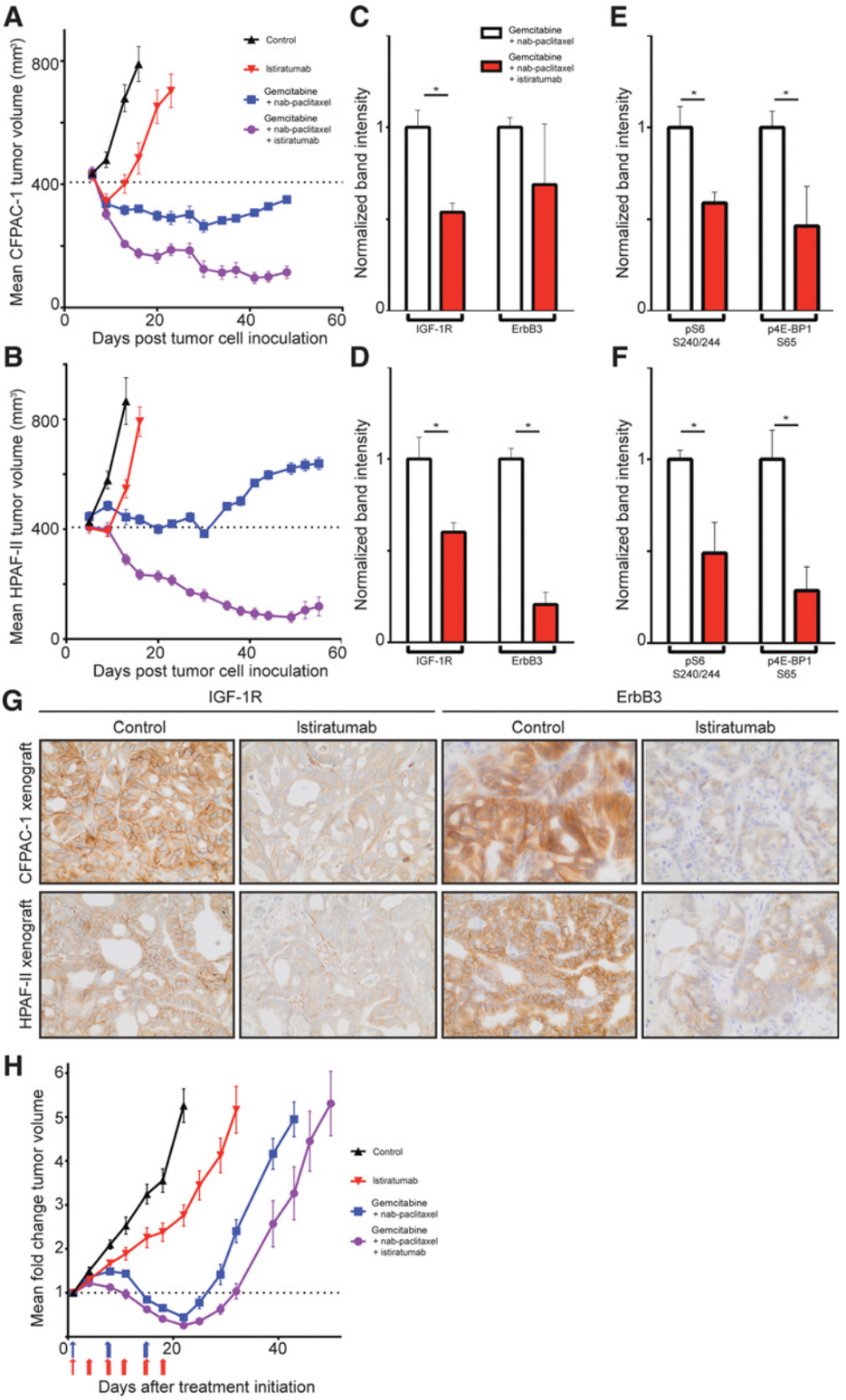

Figure 6.

Istiratumab enhances *in vivo* activity of chemotherapy in pancreatic cancer xenograft models. **A** and **B**, Addition of istiratumab to gemcitabine/nab-paclitaxel chemotherapy resulted in increased CFPAC-1 (**A**) and HPAF-II (**B**) xenograft tumor regression. Mice were treated by intraperitoneal injection with vehicle (black), istiratumab monotherapy (30 mg/kg, every 3 days; red), the dual combination of gemcitabine (10 mg/kg for CFPAC-1 and 40 mg/kg for HPAF-II, every 6 days) and nab-paclitaxel (10 mg/kg, every 3 days; blue), or the triple combination of gemcitabine, nab-paclitaxel plus istiratumab as dosed for the monotherapy (purple). Error bars represent the SEM ($N = 10$ mice, $P < 0.002$ for gemcitabine/nab-paclitaxel vs. istiratumab/gemcitabine/nab-paclitaxel from day 13 onward in both models). **C–F**, Dual IGF-1R/ErbB3 inhibition with istiratumab induces degradation of IGF-1R and ErbB3 and inhibits downstream prosurvival signaling in mouse xenograft pancreatic tumors. CFPAC-1 (**C** and **E**) and HPAF-II (**D** and **F**) end-of-study tumors were harvested 24 hours after final drug administration. Tumor lysates were immunoblotted for total IGF-1R and ErbB3 (**C** and **D**), or pS6 (S240/244) and p4E-BP1 (S65; **E** and **F**). Bars shown in red represent samples treated with istiratumab. Bar graphs represent the mean signal + SD ($N = 4$ mice), normalized to beta-actin. *, $P < 0.05$. **G,** Mice bearing CFPAC-1 and HPAF-II xenograft tumors were treated with istiratumab (30 mg/kg, i.p.), and tumors were harvested 24 hours after treatment (top two rows). Formalin-fixed, paraffin-embedded tumor samples were probed for IGF-1R or ErbB3 receptor expression by IHC. Images were acquired at 40× magnification. **H,** Addition of istiratumab to gemcitabine/nab-paclitaxel chemotherapy resulted in increased efficacy in pancreatic PDX model #14244. Mice were treated with vehicle (black), istiratumab monotherapy (30 mg/kg, twice weekly; red arrows), the dual combination of gemcitabine (25 mg/kg, weekly), and nab-paclitaxel (15 mg/kg, weekly; blue arrows), or the triple combination of gemcitabine and nab-paclitaxel (as dosed for the monotherapies) plus istiratumab (purple) for 3 weeks. Error bars represent the SEM ($N = 8$ mice).

demonstrated that the addition of a single dose of istiratumab to the dual chemotherapy regimen resulted in reduction of IGF-1R and ErbB3 at all time points (Supplementary Fig. S6).

The *in vivo* activity of the dual IGF-1R/ErbB3 inhibitor istiratumab was also investigated in a PDX model of human pancreatic cancer (PDX #14244). Istiratumab monotherapy

significantly delayed tumor growth, compared to control animals (Fig. 6H). Moreover, the addition of istiratumab improved the activity of gemcitabine/nab-paclitaxel chemotherapy (Fig. 6H). Although the magnitude of the impact of istiratumab upon chemotherapy was smaller compared to the CFPAC-1 and HPAF-II models, the improvement in tumor growth/response when istiratumab was added to chemotherapy was significant for all time points. Because the strong response of the 14244 PDX model to chemotherapy alone, treatment was stopped after three treatment cycles (week 3) and tumor regrowth posttreatment discontinuation was monitored over time. Of note, tumor regrowth was significantly slower in the animals previously treated with chemotherapy plus istiratumab, compared to chemotherapy alone (Fig. 6H).

Discussion

Poor clinical outcomes underscore the need to develop novel therapies for the treatment of pancreatic cancer. To this end, a better understanding of resistance mechanisms to standard-of-care treatment is essential. In recent years, RTKs have been identified as critical effectors of pancreatic cancer progression (27). Among them, the IGF-1R pathway has been identified as promoting prosurvival signaling and reducing the activity of cytotoxic therapies (28–30). However, scientific evidence suggests that multiple signaling pathways are dysregulated in pancreatic cancer, limiting the potential of single pathway inhibitors to control disease progression (27, 31). Here, we show that the HRG/ErbB3 axis is critically involved in pancreatic cancer and that resistance to IGF-1R signaling inhibition may be due to compensatory activation of ErbB3 downstream signaling.

In contrast to other ErbB family members, ErbB3 lacks a functioning kinase domain (32). The growth factor heregulin promotes heterodimerization of ErbB3 with other RTKs and subsequent downstream signaling activation (33). ErbB3 heterodimers are considered potent inducers of the prosurvival PI3K/AKT pathway, promoting tolerance/resistance to various standard-of-care therapies, such as PI3K signaling inhibitors, cytotoxic chemotherapies, and hormonal therapies (34). ErbB3-mediated resistance involves protein overexpression through increased *ERBB3* transcription and/or activation through increased autocrine or paracrine HRG signaling, as well as ligand-independent activation by other RTKs (35–37). Ligand-independent activation of ErbB3 may also be promoted by mutations in the extracellular domain of the protein (38). Recent evidence suggests that the tumor microenvironment can cause *de novo* resistance to PI3K signaling inhibitors by activating the HRG/ErbB3 axis (39). Using an unbiased *in vitro* growth factor screen on nine different pancreatic cancer cell lines, we show that HRG is a dominant activator of PI3K/AKT signaling in PDAC, in addition to IGF-1. Moreover, by IHC and ISH we observed that ErbB3 and/or HRG are expressed in a significant proportion of samples from patients with metastatic pancreatic cancer. These results are consistent with findings from previous studies, which showed that ErbB3 is involved in pancreatic cancer tumorigenesis (40). In addition, previous tumor microenvironment studies revealed that pancreatic cancer-associated fibroblasts can secrete heregulin, and promote the proliferation of PDAC cells by activation of ErbB3 and AKT signaling (41).

Understanding the interactions between multiple signaling pathways is critical for the identification of effective therapeutic strategies in pancreatic cancer. This has become increasingly clear as promising monospecific targeted therapies have demonstrated disappointing results in clinical trials (19, 42). It has been hypothesized that these therapies may be too narrowly focused since there are redundant, parallel signaling pathways that allow tumor cells to escape treatment. Understanding the interplay between multiple oncogenic signaling pathways in a specific tumor type is essential for the design of more effective, multi-targeted therapeutic regimens. Our study provides evidence for an interplay between IGF-1R and ErbB3 in pancreatic cancer. Consistent with previous findings (21, 43), we show that ErbB3 upregulation may compensate for IGF-1R blockade and vice versa. Moreover, our data suggest that standard-of-care chemotherapies, such as gemcitabine and paclitaxel, increase the expression and activation of both IGF-1R and ErbB3 in pancreatic cancer cells, rendering them tolerant to cytotoxic therapies. An association between decreased overall survival in stage IV metastatic pancreatic cancer patients and coexpression of IGF-1R and ErbB3 has been reported (44). Together, these findings point to ErbB3 as a potentially critical mediator of tumor growth and resistance to both IGF-1R inhibitors and chemotherapy in pancreatic cancer.

Based on the role of ErbB3 in therapy tolerance/resistance, we hypothesized that co-inhibition of IGF-1R and ErbB3 is necessary to achieve sustained suppression of pancreatic tumor growth. This hypothesis was tested using istiratumab, a fully human bispecific tetravalent IGF-1R- and ErbB3-targeting antibody, which is composed of a monoclonal IgG1 antibody, engineered to contain two single-chain Fv fragments at the carboxy termini of the heavy chain (21, 43, 45). Istiratumab possesses four high-affinity binding sites and has two modes of action: (i) it blocks IGF-1, IGF-2, and HRG binding to their receptors; and (ii) it induces degradation of receptor complexes containing IGF-1R and ErbB3 (21, 45). Our data indicate that the addition of istiratumab to the gemcitabine and (nab-)paclitaxel regimen creates a potent therapeutic opportunity in a growth factor positive setting by blocking ligand-induced IGF-1R and ErbB3 signaling and preventing chemotherapy-mediated upregulation of targeted receptors. Importantly, growth factor-induced chemoresistance was antagonized by istiratumab regardless of activating *KRAS* mutations, highlighting the importance of PI3K/AKT signaling blockade in pancreatic cancer. The choice of the bispecific drug versus monospecific antibodies was based on previous experimental and modeling analyses, which indicated a stronger suppression of AKT phosphorylation for the bispecific inhibitor, compared to a mixture of monospecific anti-IGF-1R and anti-ErbB3 antibodies at equimolar concentrations, a result that was confirmed in pancreatic cancer in the present study (21).

The *in vivo* activity of the dual IGF-1R/ErbB3 inhibitor alone was modest and varied in the different preclinical models. This could be due to variable levels of intrinsic tumor dependency to IGF-1R/ErbB3 pathway signaling. In all models, however, istiratumab enhanced the antitumor activity of chemotherapy. Our data suggest that this is likely due to chemotherapy-mediated alterations of the IGF-1R/ErbB3 pathways, such as chemotherapy-induced increase of IGF-1R and/or ErbB3 expression and activation in the presence of their ligands. The fact that istiratumab seems to be more effective when combined with chemotherapy could, however, also be explained by chemotherapy-mediated changes in the tumor microenvironment that facilitate the delivery of the antibody. Pancreatic ductal adenocarcinomas are characterized by high levels of desmoplasia, which affects the physical

properties of tumors and results in intratumor vasculature collapse (46, 47). Various drugs, including taxane-based chemotherapies, have been shown to alleviate physical forces in tumors leading to vessel deformation and improved perfusion and drug delivery (48–51). Therefore, the activity of istiratumab could be also potentiated by chemotherapy-mediated cell-killing that alters the tumor mechanopathology and improves the delivery and tumor penetration of the antibody.

The failure of monospecific IGF-1R blocking antibodies in clinical trials may have various explanations: (i) monospecific antibodies are unable to effectively inhibit IGF-1R signaling in the tumor; (ii) they are unable to inhibit the compensatory ErbB3 pathway, which reactivates AKT signaling; and (iii) they may not have been administered to the right patient population. Istiratumab degrades IGF-1R levels to a greater extent than monospecific anti-IGF-1R antibodies and prevents compensatory upregulation of ErbB3 in response to the IGF-1R blockade. Moreover, istiratumab blocks HRG signaling, which seems to be a prominent, previously overlooked activator of AKT in pancreatic cancer cells. Interestingly, IGF-1R and ErbB3 expression was not consistently elevated in the cell lines most responsive to IGF-1 and/or HRG, suggesting receptor expression alone may not be predictive of active signaling. This is consistent with previous studies showing that IGF-1R levels in patient tumor samples do not correlate with response to IGF-1R blockers (52). Of note, both IGF-1 and HRG desensitize tumor cells to gemcitabine and paclitaxel suggesting that patients with pancreatic tumors that have active IGF-1 and/or HRG signaling are more likely to respond to an IGF-1R and ErbB3 multitargeted therapy. This creates a strong rationale for using ligand levels as biomarkers in clinical trials of istiratumab. Based on these findings, a double-blind placebo-controlled phase II study of istiratumab in combination with nab-paclitaxel plus gemcitabine versus nab-paclitaxel and gemcitabine alone in front-line metastatic pancreatic cancer patients with high free IGF-1 serum levels was initiated and is currently ongoing (www.clinicaltrials.gov; ID: NCT02399137). In addition to prospective free IGF-1–based patient selection, a co-primary endpoint in the phase II proof-of-concept trial is PFS activity of istiratumab with gemcitabine/nab-paclitaxel in patients with both high free IGF-1 serum levels and heregulin-positive tumors.

In summary, our results show that the HRG/ErbB3 axis is critical to pancreatic cancer progression and therapeutic resistance to IGF-1R inhibition. Both IGF-1R and ErbB3 can serve as drivers of tumor growth and resistance/tolerance to standard-of-care chemotherapy. These data highlight that pancreatic tumors exploit both pre-wired and acquired mechanisms of activating the IGF-1R/ErbB3/AKT signaling axis to escape the cytotoxic action of standard-of-care therapies. Our findings support current clinical investigation of istiratumab in combination with gemcitabine and nab-paclitaxel in subsets of pancreatic cancer patients whose disease is characterized by high expression of IGF-1R and ErbB3 ligands.

Disclosure of Potential Conflicts of Interest

E.A. Pace and C.U. Louis are employees of Celgene Corporation. A.J. Camblin, D.C. Drummond, U.B. Nielsen, B. Schoeberl, and A.A. Lugovskoy hold ownership interest (including patents) in Merrimack Pharmaceuticals, Inc. No potential conflicts of interest were disclosed by the other authors.

Authors' Contributions

Conception and design: A.J. Camblin, E.A. Pace, S. Adams, M.D. Curley, V. Rimkunas, L. Nie, G. Tan, A. Czibere, D.C. Drummond, B. Schoeberl, V. Askoxylakis, A.A. Lugovskoy

Development of methodology: A.J. Camblin, E.A. Pace, S. Adams, V. Rimkunas, L. Nie, G. Tan, T. Bloom, D.C. Drummond, V. Askoxylakis, A.A. Lugovskoy

Acquisition of data (provided animals, acquired and managed patients, provided facilities, etc.): A.J. Camblin, E.A. Pace, S. Adams, M.D. Curley, L. Nie, G. Tan, J. Baum, C. Minx, V. Askoxylakis

Analysis and interpretation of data (e.g., statistical analysis, biostatistics, computational analysis): A.J. Camblin, E.A. Pace, S. Adams, M.D. Curley, V. Rimkunas, L. Nie, S. Iadevaia, J. Baum, A. Czibere, C.U. Louis, D.C. Drummond, J.M. Pipas, R.M. Straubinger, V. Askoxylakis, A.A. Lugovskoy

Writing, review, and/or revision of the manuscript: A.J. Camblin, E.A. Pace, S. Adams, M.D. Curley, V. Rimkunas, L. Nie, S. Iadevaia, J. Baum, A. Czibere, C.U. Louis, D.C. Drummond, B. Schoeberl, J.M. Pipas, R.M. Straubinger, V. Askoxylakis, A.A. Lugovskoy

Administrative, technical, or material support (i.e., reporting or organizing data, constructing databases): A.J. Camblin, E.A. Pace, S. Adams, G. Tan, B. Schoeberl, V. Askoxylakis, A.A. Lugovskoy

Study supervision: E.A. Pace, S. Adams, C.U. Louis, U.B. Nielsen, V. Askoxylakis, A.A. Lugovskoy

Acknowledgments

This research was funded by Merrimack Pharmaceuticals, Inc. The authors thank Dr. Gavin MacBeath, Dr. Ben Wolf, Dr. Sergio Santillana, Dr. Alena Zalutskaya, Michael Slater, and Kerry Horgan for critical discussion and review of the manuscript.

The costs of publication of this article were defrayed in part by the payment of page charges. This article must therefore be hereby marked *advertisement* in accordance with 18 U.S.C. Section 1734 solely to indicate this fact.

Received August 3, 2017; revised January 29, 2018; accepted March 12, 2018; published first March 16, 2018.

References

1. American Cancer Society. Cancer facts & figures [Internet]. Atlanta, GA: American Cancer Society; 2015. Available from: www.cancer.org.
2. Shin EJ, Canto MI. Pancreatic cancer screening. Gastroenterol Clin North Am 2012;41:143–57.
3. Von Hoff DD, Ervin T, Arena FP, Chiorean EG, Infante J, Moore M, et al. Increased survival in pancreatic cancer with nab-paclitaxel plus gemcitabine. N Engl J Med 2013;369:1691–703.
4. Conroy T, Desseigne F, Ychou M, Bouché O, Guimbaud R, Bécouarn Y, et al. FOLFIRINOX versus gemcitabine for metastatic pancreatic cancer. N Engl J Med 2011;364:1817–25.
5. Ko AH. Nanomedicine developments in the treatment of metastatic pancreatic cancer: focus on nanoliposomal irinotecan. Int J Nanomedicine 2016;11:1225–35.
6. Wang-Gillam A, Li C-P, Bodoky G, Dean A, Shan Y-S, Jameson G, et al. Nanoliposomal irinotecan with fluorouracil and folinic acid in metastatic pancreatic cancer after previous gemcitabine-based therapy (NAPOLI-1): a global, randomised, open-label, phase 3 trial. Lancet 2016;387:545–57.
7. Kurmasheva RT, Houghton PJ. IGF-I mediated survival pathways in normal and malignant cells. Biochim Biophys Acta Rev Cancer 2006;1766:1–22.
8. Li R, Pourpak A, Morris SW. Inhibition of the insulin-like growth factor-1 receptor (IGF1R) tyrosine kinase as a novel cancer therapy approach. J Med Chem 2009;52:4981–5004.
9. Pollak MN, Schernhammer ES, Hankinson SE. Insulin-like growth factors and neoplasia. Nat Rev Cancer 2004;4:505–18.

10. Chan JM, Stampfer MJ, Giovannucci E, Gann PH, Ma J, Wilkinson P, et al. Plasma insulin-like growth factor-I and prostate cancer risk: a prospective study. Science 1998;279:563–6.
11. Adachi Y, Ohashi H, Imsumran A, Yamamoto H, Matsunaga Y, Taniguchi H, et al. The effect of IGF-I receptor blockade for human esophageal squamous cell carcinoma and adenocarcinoma. Tumour Biol 2014;35: 973–85.
12. Hankinson SE, Willett WC, Colditz GA, Hunter DJ, Michaud DS, Deroo B, et al. Circulating concentrations of insulin-like growth factor-I and risk of breast cancer. Lancet 1998;351:1393–6.
13. Liu Y-C, Leu C-M, Wong F-H, Fong W-S, Chen S-C, Chang C, et al. Autocrine stimulation by insulin-like growth factor I is involved in the growth, tumorigenicity and chemoresistance of human esophageal carcinoma cells. J Biomed Sci 2002;9:665–74.
14. Ma J, Pollak MN, Giovannucci E, Chan JM, Tao Y, Hennekens CH, et al. Prospective study of colorectal cancer risk in men and plasma levels of insulin-like growth factor (IGF)-I and IGF-binding protein-3. J Natl Cancer Inst 1999;91:620–5.
15. Dziadziuszko R, Camidge DR, Hirsch FR. The insulin-like growth factor pathway in lung cancer. J Thorac Oncol 2008;3:815–8.
16. Jiang B, Gu Y, Chen Y. Identification of novel predictive markers for the prognosis of pancreatic ductal adenocarcinoma. Cancer Invest 2014;32: 218–25.
17. Hirakawa T, Yashiro M, Murata A, Hirata K, Kimura K, Amano R, et al. IGF-1 receptor and IGF binding protein-3 might predict prognosis of patients with resectable pancreatic cancer. BMC Cancer 2013;13:392.
18. Kindler HL, Richards DA, Garbo LE, Garon EB, Stephenson JJ, Rocha-Lima CM, et al. A randomized, placebo-controlled phase 2 study of ganitumab (AMG 479) or conatumumab (AMG 655) in combination with gemcitabine in patients with metastatic pancreatic cancer. Ann Oncol Off J Eur Soc Med Oncol 2012;23: 2834–42.
19. McCaffery I, Tudor Y, Deng H, Tang R, Suzuki S, Badola S, et al. Putative predictive biomarkers of survival in patients with metastatic pancreatic adenocarcinoma treated with gemcitabine and ganitumab, an IGF1R inhibitor. Clin Cancer Res 2013;19:4282–9.
20. Fuchs CS, Azevedo S, Okusaka T, Van Laethem J-L, Lipton LR, Riess H, et al. A phase 3 randomized, double-blind, placebo-controlled trial of ganitumab or placebo in combination with gemcitabine as first-line therapy for metastatic adenocarcinoma of the pancreas: the GAMMA trial. Ann Oncol 2015;26:921–7.
21. Fitzgerald JB, Johnson BW, Baum J, Adams S, Iadevaia S, Tang J, et al. MM-141, an IGF-IR- and ErbB3-directed bispecific antibody, overcomes network adaptations that limit activity of IGF-IR inhibitors. Mol Cancer Ther 2014;13:410–25.
22. Huang X, Gao L, Wang S, McManaman JL, Thor AD, Yang X, et al. Heterotrimerization of the growth factor receptors erbB2, erbB3, and insulin-like growth factor-i receptor in breast cancer cells resistant to herceptin. Cancer Res 2010;70:1204–14.
23. Knowlden JM, Gee JMW, Barrow D, Robertson JF, Ellis IO, Nicholson RI, et al. erbB3 recruitment of insulin receptor substrate 1 modulates insulin-like growth factor receptor signalling in oestrogen receptor-positive breast cancer cell lines. Breast Cancer Res 2011;13:R93.
24. Jia Y, Zhang Y, Qiao C, Liu G, Zhao Q, Zhou T, et al. IGF-1R and ErbB3/HER3 contribute to enhanced proliferation and carcinogenesis in trastuzumab-resistant ovarian cancer model. Biochem Biophys Res Commun 2013;436:740–5.
25. Zhang Z, Wang J, Ji D, Wang C, Liu R, Wu Z, et al. Functional genetic approach identifies MET, HER3, IGF1R, INSR pathways as determinants of lapatinib unresponsiveness in HER2-positive gastric cancer. Clin Cancer Res 2014;20:4559–73.
26. Eser S, Schnieke A, Schneider G, Saur D. Oncogenic KRAS signalling in pancreatic cancer. Br J Cancer 2014;111:817–22.
27. Preis M, Korc M. Kinase signaling pathways as targets for intervention in pancreatic cancer. Cancer Biol Ther 2010;9:754–63.
28. Kawanami T, Takiguchi S, Ikeda N, Funakoshi A. A humanized anti-IGF-1R monoclonal antibody (R1507) and/or metformin enhance gemcitabine-induced apoptosis in pancreatic cancer cells. Oncol Rep 2012;27:867–72.
29. Tian X, Hao K, Qin C, Xie K, Xie X, Yang Y. Insulin-like growth factor 1 receptor promotes the growth and chemoresistance of pancreatic cancer. Dig Dis Sci 2013;58:2705–12.
30. Ireland L, Santos A, Ahmed MS, Rainer C, Nielsen SR, Quaranta V, et al. Chemoresistance in pancreatic cancer is driven by stroma-derived insulin-like growth factors. Cancer Res 2016;76:6851–63.
31. Jones S, Zhang X, Parsons DW, Lin JC-H, Leary RJ, Angenendt P, et al. Core signaling pathways in human pancreatic cancers revealed by global genomic analyses. Science 2008;321:1801–6.
32. Jura N, Shan Y, Cao X, Shaw DE, Kuriyan J. Structural analysis of the catalytically inactive kinase domain of the human EGF receptor 3. Proc Natl Acad Sci U S A 2009;106:21608–13.
33. Wallasch C, Weiss FU, Niederfellner G, Jallal B, Issing W, Ullrich A. Heregulin-dependent regulation of HER2/neu oncogenic signaling by heterodimerization with HER3. EMBO J 1995;14:4267–75.
34. Schoeberl B, Kudla A, Masson K, Kalra A, Curley M, Finn G, et al. Systems biology driving drug development: from design to the clinical testing of the anti-ErbB3 antibody seribantumab (MM-121). NPJ Syst Biol Appl 2017;3:16034.
35. Garrett JT, Olivares MG, Rinehart C, Granja-Ingram ND, Sánchez V, Chakrabarty A, et al. Transcriptional and posttranslational up-regulation of HER3 (ErbB3) compensates for inhibition of the HER2 tyrosine kinase. Proc Natl Acad Sci U S A 2011;108:5021–6.
36. Engelman JA, Zejnullahu K, Mitsudomi T, Song Y, Hyland C, Park JO, et al. MET amplification leads to gefitinib resistance in lung cancer by activating ERBB3 signaling. Science 2007;316:1039–43.
37. Sergina N V, Rausch M, Wang D, Blair J, Hann B, Shokat KM, et al. Escape from HER-family tyrosine kinase inhibitor therapy by the kinase-inactive HER3. Nature 2007;445:437–41.
38. Arteaga CL, Engelman JA. ERBB receptors: from oncogene discovery to basic science to mechanism-based cancer therapeutics. Cancer Cell 2014;25:282–303.
39. Kodack DP, Askoxylakis V, Ferraro GB, Sheng Q, Badeaux M, Goel S, et al. The brain microenvironment mediates resistance in luminal breast cancer to PI3K inhibition through HER3 activation. Sci Transl Med 2017;9: eaal4682.
40. Liles JS, Arnoletti JP, Tzeng C-WD, Howard JH, Kossenkov AV, Kulesza P, et al. ErbB3 expression promotes tumorigenesis in pancreatic adenocarcinoma. Cancer Biol Ther 2010;10:555–63.
41. Liles JS, Arnoletti JP, Kossenkov AV, Mikhaylina A, Frost AR, Kulesza P, et al. Targeting ErbB3-mediated stromal-epithelial interactions in pancreatic ductal adenocarcinoma. Br J Cancer 2011;105:523–33.
42. Philip PA, Goldman B, Ramanathan RK, Lenz H-J, Lowy AM, Whitehead RP, et al. Dual blockade of epidermal growth factor receptor and insulin-like growth factor receptor-1 signaling in metastatic pancreatic cancer: phase Ib and randomized phase II trial of gemcitabine, erlotinib, and cixutumumab versus gemcitabine plus erlotinib. Cancer 2014;120: 2980–5.
43. Fitzgerald J, Lugovskoy A. Rational engineering of antibody therapeutics targeting multiple oncogene pathways. MAbs 2011;3: 299–309.
44. Wang-Gillam A, Rimkunas V, Abu-Yousif AO, Nywening T, Gao F, DeNardo DG, et al. HER3 as a potential prognostic biomarker in pancreatic cancer. J Clin Oncol 2015;33s:(suppl; abst 295).
45. Xu L, Kohli N, Rennard R, Jiao Y, Razlog M, Zhang K, et al. Rapid optimization and prototyping for therapeutic antibody-like molecules. MAbs 2013;5:237–54.
46. Stylianopoulos T, Jain RK. Combining two strategies to improve perfusion and drug delivery in solid tumors. Proc Natl Acad Sci 2013; 110:18632–7.
47. Jain RK, Martin JD, Stylianopoulos T. The role of mechanical forces in tumor growth and therapy. Ann Rev Biomed Eng 2014; 16:321–46.
48. Griffon-Etienne G, Boucher Y, Brekken C, Suit HD, Jain RK. Taxane-induced apoptosis decompresses blood vessels and lowers interstitial fluid pressure in solid tumors: clinical implications. Cancer Res 1999; 59:3776–82.
49. Chauhan VP, Martin JD, Liu H, Lacorre DA, Jain SR, Kozin SV, et al. Angiotensin inhibition enhances drug delivery and potentiates chemotherapy by decompressing tumour blood vessels. Nat Commun 2013; 4:2516.

50. Olive KP, Jacobetz MA, Davidson CJ, Gopinathan A, McIntyre D, Honess D, et al. Inhibition of Hedgehog signaling enhances delivery of chemotherapy in a mouse model of pancreatic cancer. Science 2009; 324:1457–61.
51. Provenzano PP, Cuevas C, Chang AE, Goel VK, Von Hoff DD, Hingorani SREnzymatic targeting of the stroma ablates physical barriers to treatment of pancreatic ductal adenocarcinoma. Cancer Cell 2012;21:418–29.
52. Cao Y, Roth M, Piperdi S, Montoya K, Sowers R, Rao P, et al. Insulin-like growth factor 1 receptor and response to anti-IGF1R antibody therapy in osteosarcoma. PLoS One 2014;9: e106249.